LIMNOLOGY and OCEANOGRAPHY

ASLO

Limnol. Oceanogr. 9999, 2020, 1–18

doi: 10.1002/lno.11626

Aufeis fields as novel groundwater-dependent ecosystems in the arctic cryosphere

Alexander D. Huryn,[1*] **Michael N. Gooseff**,[2] **Patrick J. Hendrickson**,[2] **Martin A. Briggs**,[3] **Ken D. Tape**,[4] **Neil C. Terry**[3]

[1]Department of Biological Sciences, University of Alabama, Tuscaloosa, Alabama
[2]Department of Civil, Environmental, and Architectural Engineering, University of Colorado, Boulder, Colorado
[3]Earth System Processes Division, U.S. Geological Survey, Storrs, Connecticut
[4]Water & Environmental Research Center, University of Alaska Fairbanks, Institute of Northern Engineering, Fairbanks, Alaska

Abstract

River *aufeis* (ow′ fīse) are widespread features of the arctic cryosphere. They form when river channels become locally restricted by ice, resulting in cycles of water overflow and freezing and the accumulation of ice, with some *aufeis* attaining areas of ~ 25 + km^2 and thicknesses of 6+ m. During winter, unfrozen sediments beneath the insulating ice layer provide perennial groundwater-habitat that is otherwise restricted in regions of continuous permafrost. Our goal was to assess whether *aufeis* facilitate the occurrence of groundwater invertebrate communities in the Arctic. We focused on a single *aufeis* ecosystem (~ 5 km^2 by late winter) along the Kuparuk River in arctic Alaska. Subsurface invertebrates were sampled during June and August 2017 from 50 3.5-cm diameter PVC wells arranged in a 5 × 10 array covering ~ 40 ha. Surface invertebrates were sampled using a quadrat approach. We documented a rich assemblage of groundwater invertebrates (49 [43–54] taxa, $\bar{X}$ [95% confidence limits]) that was distributed below the sediment surface to a mean depth of ~ 69 ± 2 cm ($\bar{X}$ ± 1 SE) throughout the entire well array. Although community structure differed significantly between groundwater and surface habitats, the taxa richness from wells and surface sediments (43 [35–48] taxa) did not differ significantly, which was surprising given lower richness in subsurface habitats of large, riverine gravel-aquifer systems shown elsewhere. This is the first demonstration of a rich and spatially extensive groundwater fauna in a region of continuous permafrost. Given the geographic extent of *aufeis* fields, localized groundwater-dependent ecosystems may be widespread in the Arctic.

River *aufeis* (ow′ fīse) are common and widespread features of the arctic cryosphere, particularly in northern Alaska and Siberia (Yoshikawa et al. 2007; Alekseyev 2015). They form when the cross-sectional area of a stream channel becomes locally restricted as ice accumulates during winter. Such restrictions or "choke-points" result in bulk overflow and local increases in hydrostatic pressure, causing water to move upward through fissures onto the original ice layer (Hall 1980; Yoshikawa et al. 2007; Alekseyev 2015). This overflowing water subsequently freezes to produce additional ice layers, thus explaining the origin of the term *aufeis*, which literally translates from German to "on ice" (von Middendorff 1867). This process, repeated through the long arctic winter, can generate large volumes of ice, with some *aufeis* in arctic Alaska—where they are also known as "icings"—attaining areas of 20 + km^2 (Hall 1980; Clark and Lauriol 1997) and localized thicknesses of 6+ m (Terry et al. 2020). The cumulative area of late-winter *aufeis* in the Sagavanirktok River drainage alone, for example, ranges from 10^2 to 10^3 km^2 (Li et al. 1997). In eastern Siberia, where *aufeis* are known as *naleds*, > 10,000 *aufeis* with a cumulative area of ~ 50,000 km^2 containing 30 km^3 of water have been documented (Sokolov 1991; Alekseyev 2015). When thawed, *aufeis* leave footprints in the form of "*aufeis* glades" (Alekseyev 2015) or, perhaps more accurately in tundra habitats, "*aufeis* barrens," because of the near absence of vascular vegetation due to ice cover during much of the growing season. *Aufeis* barrens are distinctive landscape features of the arctic tundra and provide reliable indicators of *aufeis* locations (Yoshikawa et al. 2007, Alekseyev 2015; A. D. Huryn, pers. obs.).

The formation of large *aufeis* requires a source of flowing water during winter, which may seem counterintuitive in

*Correspondence: huryn@bama.ua.edu

Additional Supporting Information may be found in the online version of this article.

regions of continuous permafrost (Brown et al. 1997; Kane et al. 2013). However, perennial and seasonal spring-streams formed from groundwater discharged through unfrozen sediments connecting the surface with sub- or intra-permafrost aquifers can be regionally abundant (Craig and McCart 1975; Childers et al. 1977). Unfrozen, intra-permafrost aquifers and the conduits of unfrozen sediments that connect both sub- and intra-permafrost aquifers to the surface are known as *taliks* (Zhang 2011; Kane et al. 2013). In cases where aquifers are seasonally depleted, *aufeis* may be relatively small (Hall 1980). In cases where flow is perennial, however, enormous *aufeis* may form (e.g., 10s of km^2 in area, Hall 1980, Alekseyev 2015). During winter, *aufeis* formed by perennial water sources overlie a "wet base" of pressurized water in the sediments below that breaches the ice layer at points of weakness, causing the accumulations of ice at the thinnest places, eventually resulting in a massive sheet of ice (Clark and Lauriol 1997; Terry et al. 2020). Unfrozen, saturated sediments beneath an *aufeis* are maintained during winter due to insulation by the ice layer, advection of heat from upwelling groundwater, and by latent heat released during freezing cycles (Hall 1979; Schohl and Ettema 1990; Clark and Lauriol 1997, Terry et al. 2020). Such perennially saturated sediments provide extensive, below-ground interstitial habitat that would otherwise be absent in regions underlain by continuous permafrost (Brown et al. 1997; Alekseyev 2015).

Although *aufeis* are prominent features of some arctic landscapes, particularly the eastern North Slope of Alaska and Siberia, they have received scant attention from ecologists. Nevertheless, they likely play regionally important roles as: (1) water sources maintaining summer stream discharge and connectivity during the summer thaw (Kane and Slaughter 1972; Li et al. 1997; Alekseyev 2015), (2) local habitat for fishes (Sandstrom 1995) and mammals (Gill and Kershaw 1981), (3) a form of disturbance that maintains characteristic plant communities (Alekseyev 2015), and (4) perennially unfrozen interstitial-groundwater habitat for groundwater invertebrate communities (Terry et al. 2020). A subsurface, freshwater fauna has been unanticipated for the Arctic due to the assumption of continuous permafrost beneath seasonally thawed, hyporheic sediments surrounding stream beds (Edwardson et al. 2003; Brosten et al. 2006; Zarnetske et al. 2008).

The richness of subsurface invertebrate communities can attain 80+ taxa (Stanford et al. 1994) in the alluvial sediments of temperate ecosystems, providing that there is a diversity of sediment patches varying in pore water volume, particulate organic matter, microbial biomass, and dissolved oxygen concentrations (Strayer et al. 1997; Robertson and Wood 2010). Such communities have been shown to be significant contributors to ecosystem processes in temperate stream ecosystems where complex food webs can connect surface and subsurface ecosystems via their role in nutrient cycling and energy flow (Stanford et al. 1994; Strayer et al. 1997; Boulton et al. 2010). Evidence for a subsurface invertebrate fauna in arctic Alaska is sparse but exists in the form of collections of stonefly (Plecoptera) species documented to be hyporheic-groundwater specialists in association with several *aufeis* fields (Kendrick and Huryn 2014). Our goal here is to comprehensively document the subsurface fauna of a single *aufeis* field and to, more generally, introduce *aufeis* fields as potentially unique and regionally important habitats for perennially active, groundwater invertebrate communities.

Methods

Study area

This study focused on a large (e.g., > 5 km^2 by late winter) *aufeis* associated with the Kuparuk River ("Kuparuk *aufeis*" hereafter, Fig. 1, 68.979442°N 149.711800°W; Yoshikawa et al. 2007, King et al. 2020, Terry et al. 2020). The Kuparuk River rises in the foothills of the Brooks Range and flows northward across the Arctic Coastal Plain to the Arctic Ocean west of Prudhoe Bay. This 8259-km^2 drainage is underlain by continuous permafrost with a thickness ranging from 300 m in the foothills to 600 m in the Arctic Coastal Plain (Collett

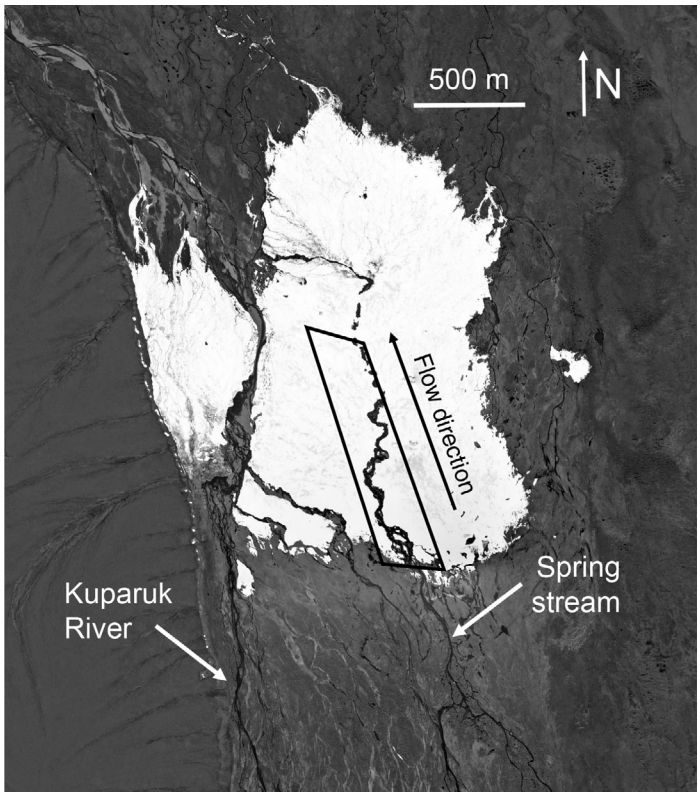

Fig. 1. Satellite image showing Kuparuk *aufeis* field on 20 June 2010 (Google Earth™, accessed 14 December 2019). Significant seasonal thawing of the *aufeis* is in progress. The quadrangle indicates the position of the well array. The general direction of surface and subsurface flow is from SSE to NNE. The Kuparuk River main channel is constrained by the bluffs to the west. The perennial spring that provides water that forms the *aufeis* during winter is indicated to the south.

et al. 1989). During summer, an active layer (i.e., layer of sediment above the permafrost that thaws and freezes each year) with a maximum depth of 0.5 to 1.0 m develops (Nelson et al. 1997). The permafrost below this active layer functions as an aquiclude with significant effects on runoff dynamics (King et al. 2020). The Kuparuk River has been subject to intensive study as part of the U.S. National Science Foundation - Long Term Ecological Research network (Bowden et al. 2014).

The area and volume of the Kuparuk *aufeis* varies seasonally, being greatest during late winter (i.e., April) when it may cover 8+ km^2 and reach thicknesses up to ~ 7 m (McNamara et al. 1998; Yoshikawa et al. 2007; Terry et al. 2020). The total volume of water retained as ice over a 10-year period ranged from 15.2 to 31.2 $\times 10^6$ m^3 (Yoshikawa et al. 2007). By September, residual ice is usually present, but the volume varies depending on meteorological conditions during summer and the amount of ice accumulated over the previous winter (Yoshikawa et al. 2007; Pavelsky and Zarnetske 2017; A. D. Huryn, pers. obs.). Like other large *aufeis* on the North Slope, the Kuparuk *aufeis* is formed from the discharge of a spring (Q ~ 459 L/s; Parker and Huryn 2013). The aquifer feeding this spring is hypothesized to be recharged from a losing reach of the Kuparuk River ~ 10+ km upstream of the *aufeis* field, a scenario supported by a recent hydrological budget for the greater Kuparuk River (King et al. 2020). This *talik* is likely structured by a subsurface paleochannel (Poole et al. 2002) that emerges on the floodplain surface as the spring's source and that is presumably a remnant of a drainage system associated with a Pleistocene glacier that terminated upstream of the present-day *aufeis* field (Hamilton 1978; Yoshikawa et al. 2007).

Terry et al. (2020) used a combination of ground-penetrating radar (GPR) and surface nuclear magnetic resonance (NMR) to survey subsurface hydrological conditions over a ~ 0.3 km^2 area of the Kuparuk *aufeis* during September 2016 (minimal ice volume, GPR only) and over a ~ 5 km^2 area during April 2017 (maximum ice volume, GPR + NMR). During September 2016, GPR detected an active layer with a depth of approximately 4 m in the northwestern area of the *aufeis* field but was unable to capture the bottom of the deeper unfrozen sediments in the central and southern areas where there is presumably more groundwater flow in the vicinity of the spring. During April 2017, GPR indicated an ice layer up to 6 m thick that overlaid frozen sediments (primarily cobbles) to a depth of 3 to 5 m, except in zones of preferential groundwater upwelling onto the surface ice pack where frozen cobbles were not apparent. Below this basal layer, GPR and NMR identified regions of *talik*. In some locations within the southern area of the *aufeis*, the base of this *talik* extended ≥ 20 m beneath the sediment surface to form an ~ 13-m thick layer of unfrozen, saturated sediments, indicating that year-round flow occurs beneath much of the *aufeis* field (Terry et al. 2020). Furthermore, discrete zones of groundwater upwelling and associated "ice blistering" (raised humps in the *aufeis* surface) indicated direct connection between the *aufeis* surface and the *talik* below (N. C. Terry, pers. obs.; A. D. Huryn, pers. obs.). These findings indicate that the Kuparuk *aufeis*-spring system maintains a significant and dynamic volume of perennially saturated sediments beneath several meters of frozen sediments during winter (Terry et al. 2020).

Well array

During mid-August 2016, 50 3.5-cm diameter PVC wells were driven into the sediments of the *aufeis* field using a gas-powered impact driver (Rhino Fence Pro GPD-40, Commerce City, Colorado) and steel insertion rod to the depth of refusal (37 to 92 cm below the sediment surface in practice, see the Results section below). The bottom rim of the well was chamfered to facilitate insertion and 24 15-mm diameter holes were drilled in the bottom 20 cm to allow horizontal movement of water and invertebrates into the well. An Onset HOBO U20-001-01 water-level and temperature logger (± 1.0 cm depth accuracy, ± 0.44°C temperature accuracy, Onset Data Loggers, Bourne, Massachusetts) or a U20L-04 water-level and temperature logger (± 0.79 cm depth accuracy, ± 0.44°C temperature accuracy) was lowered to the base of each well and secured to the well's cap with a nylon cord. Data were collected at 30-min intervals from mid-August 2016 through mid-August 2017 (Gooseff and Huryn 2019; Terry et al. 2019). The resulting well array was arranged in a grid with 10 transects (5 wells each) spaced at ~ 150-m intervals latitudinally and 5 transects (10 wells each) spaced at ~ 75-m intervals longitudinally. This grid was positioned to capture a primary surface-flow channel and extended from the spring-stream complex at the southern edge of the field to the residual ice layer at the northern edge of the field. The grid dimensions were ~ 1300 m N-S × 300 m E-W. The coordinates of the southeastern and northwestern corners of the grid were 68.967617°N, 149.700808°W and 68.969016°N, 149.714128°W, respectively (Fig. 1). The general relationship between the well array and the subsurface hydrology of the Kuparuk *aufeis* field is provided graphically as fig. 11 in Terry et al. (2020).

Hyporheic vs. groundwater zones

The hydrogeological framework of the Kuparuk *aufeis* field is complex, being composed of a three-dimensional network of subsurface flow paths beneath and parallel to surface channels likely carrying surface water and admixtures of surface water combined with upwelling hyporheic water and/or groundwater (Terry et al. 2020). The breadth (e.g., perpendicular to mean direction of flow) of this network may be hundreds of meters in extent and 10+ meters in depth (Terry et al. 2020). Some of the wells in the array were likely placed within true hyporheic zones (i.e., containing subsurface water actively exchanged with surface water) while others were likely placed within flow pathways containing groundwater (i.e., water that has not yet mixed with surface water at the *aufeis* field). Consequently, we

follow Woessner (2017) in using the more general term "groundwater" to refer to the saturated zones of the subsurface sediments of the *aufeis* field, except in cases where water-mixing dynamics can be definitively identified.

Water chemistry, invertebrates, and apparent hydraulic conductivity

Once the well array was installed, wells were overwintered beneath the *aufeis* and sampled as early in the year as practical (i.e., when exposed following thaw, mid-June 2017) and during mid-August 2017 when only residual ice remained. Sampling consisted of pumping a known volume of water (10.9 liters) from the well into a graduated bucket using a hand-operated pump (Wastecorp Sludge Sucker Professional Hand Pump - 5.5 cm, Model No. 63839–20, Wastecorp Pumps, Depew, New York). This sample volume was based on the recommendations of Boulton et al. (2004) and Kibichii et al. (2009) who suggested that volumes of 3 to 10 liters provided consistent invertebrate assemblage compositions in their studies which involved sampling interstitial water from hyporheic sediments using a pump-based approach. Given a volume of 10.9 liters of water pumped from each well and a maximum well volume (i.e., 96 cm length of 3.5-cm diameter PVC tubing) of 0.92 liters, the ratio of interstitial water to unpurged well water was a minimum of $\sim 12:1$, or ~ 10 liters of interstitial water per sample.

Following pumping of each well, five 50-mL samples of water were removed from the bucket and filtered through pre-ashed GF/C glass fiber filters for later analyses of NH_4—N, NO_3—N, NO_2—N and soluble reactive phosphorus (SRP, PO_4—P) using a Lachat Quickchem FIA + 8000 Series flow injection analyzer (Hach Company, Loveland, Colorado). These samples were stored on ice while in the field and then frozen until analysis. Concentrations of dissolved oxygen (DO, mg DO l^{-1}, % saturation) and specific conductance (SpC, μS cm^{-1}) were then measured within the well and in nearby surface water habitats, where possible, using hand-held meters (YSI Incorporated, Yellow Springs, Ohio). Once sampling for water chemistry was completed, the remaining contents of the bucket were filtered through a 250-μm sieve and preserved with $\sim 4\%$ formaldehyde until laboratory processing, which consisted of rinsing the sample through nested sieves (250–1000 μm) and removing the invertebrates from each size fraction by hand under a dissecting microscope. Except for the Ostracoda, Cladocera, and Copepoda, further processing consisted of identifying specimens to the lowest practical taxonomic level, usually genus (Stewart and Oswood 2006; Anderson et al. 2013; Merritt et al. 2019). Larvae of the Chironomidae were slide-mounted using CMC-10 (Masters Company) prior to identification. The Ostracoda, Cladocera and Copepoda were identified by Limnopro Aquatic Sciences (https://www.limnopro.com/). Once invertebrates were removed from samples, the remaining particulate material was dried at 50°C to a constant mass (> 48 h), weighed (= dry mass), combusted (500°C), and reweighed (= ash mass). The organic matter content of the sample was calculated as the difference between dry mass and ash mass.

Once sampling of invertebrates was completed, the turnover time for the volume of well water was measured by injecting 60 mL of saturated NaCl solution into each well, measuring SpC (Onset HOBO U24-001, accuracy ± 5 μS cm^{-1}, Onset Data Loggers) at 30 s intervals for 5 min, and fitting a negative exponential model to the resulting data (least-squares regression), the exponent of which provided a proportional water exchange coefficient (i.e., proportion of well volume s^{-1}). This coefficient was then combined with well dimensions to estimate hydraulic conductivity as the apparent velocity of water assumed to be moving perpendicular to the well (apparent hydraulic conductivity, m 24 h^{-1} = m d^{-1}).

Invertebrates from surface sediments were sampled during mid-August 2017. One sample was taken at each of the 10 E-W well transects (spaced at 150-m intervals, see the Well array section above) as close to the center well as practical (i.e., closest surface channel) using a Surber sampler (0.09 m^2, 243-μm mesh, $N = 10$). Cobble-sized particles were removed from the sampler frame and scrubbed in a bucket using a nylon brush. The remaining particles within the sample frame were then agitated to entrain organic materials into the capture net. The contents of the net were combined with organic matter sieved (250 μm) from the bucket and preserved with $\sim 4\%$ formaldehyde until laboratory processing. Five 50-mL samples of water were also collected at each sampling location and filtered through pre-ashed GF/C glass fiber filters for later nutrient analyses.

Statistical analysis of temporal and spatial patterns of invertebrate assemblages

Temporal and spatial patterns of invertebrate community structure were analyzed using non-metric multi-dimensional scaling (nMDS), followed by ANOSIM (999 permutations) and SIMPER analyses (PRIMER, version 6, Clarke and Gorley 2006). ANOSIM ("analysis of similarity") is analogous to one- and two-way ANOVA and is used to test hypotheses about multivariate differences between groups of samples (Clarke and Gorley 2006). Following a significant result from ANOSIM, SIMPER ("similarity percentages" analysis) may be used to assess the relative importance of different taxa in driving such differences (Clarke and Gorley 2006). Prior to analysis, data were fourth-root transformed and taxa occurring in < 3 samples were removed based on the assumption that taxa collected from only one or two wells would provide little information regarding the spatial distribution of subsurface fauna within the well grid. In practice, resulting nMDS plots showed little discernable change following the removal of taxa occurring in < 5 wells. Differences between either numerical or proportional abundance of dominant invertebrate taxa (i.e., those taxa cumulatively contributing $\sim 80\%$ total mean Bray–Curtis dissimilarity) between temporal or spatial

elements of the well array or between habitats (i.e., surface sediment vs. wells) were further assessed using nonparametric two-sample randomization test (Manly 1991; Benke and Huryn 2006) if ANOSIM indicated a significant global difference. The two-sample randomization test was based on estimates of invertebrate abundance and richness using a bootstrapping approach, where the original data were randomly resampled with replacement to produce vectors of 1000 bootstrapped means. These vectors were also used to estimate mean abundance and richness and, when sorted from smallest to greatest value, nonparametric 95% confidence limits estimated as the 2.5^{th} and 97.5^{th} percentiles. Given the exploratory nature of the study, a nominal p value of 0.05 was used for post hoc comparisons to minimize Type II error (i.e., a procedure such as the Bonferroni correction was not adopted, Day and Quinn 1989; Rothman 1990; Savitz and Olshan 1995). Prior to analyses, well invertebrate abundance and organic matter estimates were standardized to 10 liters. Except for a single well (Well 4), the full sample of 10.9 liters of water was obtained, which effectively eliminated problems related to the effect of varying sample volumes on perceived invertebrate abundance and assemblage structure.

Comparisons of taxonomic richness and structure between well and surficial sediment assemblages are problematical due to substantial differences in physical context (e.g., unspecified spatial dimensions for well samples, unknown differences in taxon-specific capture probabilities between well samples vs. surface sediments). In addition to these considerations, it should also be noted that the installation of the well using an impact driver and steel insertion rod also likely affected local sediment characteristics and potentially habitat attributes that may further bias findings. Nevertheless, an attempt to provide insight into differences in relative taxonomic assemblage structure and richness of surface and subsurface invertebrates was made using comparison of proportional abundance and sample-based rarefaction (Gotelli and Colwell 2011). Comparisons of proportional abundance were conducted using ANOSIM and SIMPER followed by pairwise comparisons, as described above. The results of these analyses should be assessed with some caution due to the potential for differing levels of taxonomic bias between habitats due to sampling methods. Sample-based rarefaction was accomplished by bootstrapping, where the original data were randomly resampled with replacement to produce 1000 vectors containing the number of taxa expected from one to the summed maximum number of samples taken from a given habitat on a given date. These data were analyzed by regressing the mean bootstrapped number of taxa against number of samples. To correct for the effect of differences in the number of individuals sample^{-1} on taxon richness, accumulated samples were converted to accumulated individuals thus allowing richness vs. number of accumulated individuals to be analyzed, as suggested by Gotelli and Colwell (2011). Differences in the slopes and intercepts of least-squares regression equations describing the relationships between taxonomic richness were assessed using General Linear Models (GLM).

Results

Well depth and temperature

During the spring thaw of 2017, five wells were damaged by collapsing ice and could not be sampled, although data from thermistors and pressure transducers were recovered from several of these. During 14–16 June 2017, the *aufeis* thawed sufficiently to allow sampling of seven wells in the southern portion of the aufeis field. During 12–17 August 2017, all 45 remaining wells were sampled. The mean depth below the sediment surface of the 45 intact wells sampled during 2017 was 68.5 ± 1.6 cm ($\bar{X}$ ±1 SE, range = 37–92 cm, Table 1). Only seven wells had depths < 60 cm. Temporal temperature and pressure records indicated that water in all wells froze or partially froze during winter 2016–2017 with the

Table 1. Summary of physical attributes of wells sampled at the Kuparuk *aufeis* field, North Slope, Alaska. Annual means are for a period from approximately 22 Aug 2016 through 22 Aug 2017. Measurements of well depth and water height were made during 12–17 Aug 2017. Negative well water heights indicate that water height is below the sediment surface. Freeze and thaw dates were estimated using data from both thermistors and pressure transducers. See the Methods section for further information.

	$\bar{X} \pm$ SE	Range	*N*
Mean well depth (cm)	68.5 ± 1.6 cm	37.0 to 92.0 cm	46
Mean well water height (cm below sediment)	−3.0 ± 1.3 cm	−27.0 to 13.0 cm	46
Mean annual well temperature (°C)	−0.4 ± −0.1	−2.5 to 1.5	47
Mean annual well temperature ≥ 0°C	3.8 ± 0.1	1.9 to 5.3	47
Mean minimum well temperature (°C)	−4.7 ± 2.6	−11.2 to 0.0	47
Mean maximum well temperature (°C)	10.0 ± 2.4	5.8 to 17.4	47
Mean # days ≥ 0°C	115 ± 6 days	65 to 293 days	47
Apparent freeze date (ordinal date)	305 ± 2	286 to 346	46*
Apparent thaw date (ordinal date)	184 ± 4	118 to 221	47

*Excluding one well with an apparent freeze date of 17 Feb 2017.

Table 2. Summary of physical and chemical attributes of water from wells sampled 12–17 Aug 2017 at the Kuparuk *aufeis* field, North Slope, Alaska. Data are shown for all wells for which data were available (N = 46, except for hydraulic conductivity where N = 38) and wells 1–15 (N = 15) and wells 16–50 (N = 31). Wells 1–15 showed significantly higher levels of specific conductance (SpC) than wells 16–50 ($p < 0.0001$).

	All wells	Wells 1–15	Wells 16–50
Specific conductance (μS cm^{-1} ± SE)	55.8 ± 3.1	84.4 ± 2.3	42.0 ± 0.6
Dissolved oxygen (mg L^{-1} ± SE)	12.2 ± 0.4	10.0 ± 0.8	13.3 ± 0.2
Dissolved oxygen (% saturation ± SE)	105.2 ± 3.2	85.3 ± 6.8	114.9 ± 1.6
Air-well temperature correlation coefficient (r ± SE)	0.23 ± 0.03	0.14 ± 0.03	0.27 ± 0.04
Apparent hydraulic conductivity (m d^{-1})	47.7 ± 8.6	35.5 ± 7.1*	54.1 ± 12.4†
Nitrate-N (μg-N L^{-1} ± SE)	98.9 ± 6.7	108.4 ± 12.9	94.4 ± 7.7
Ammonium-N (μg-N L^{-1} ± SE)	6.3 ± 1.6	5.9 ± 0.8	6.5 ± 2.3
SRP (μg-P L^{-1} ± SE)	4.3 ± 0.2	4.6 ± 0.4	4.1 ± 0.2

*N = 13.
†N = 25.

onset and duration of freezing varying with location. This result was consistent with the April 2017 geophysical mapping of the *aufeis* field by Terry et al. (2020). A significant trend toward later freezing in the northern portions of the well array was detected (R^2 = 0.47, p < 0.0001, F = 38.4, N = 46). Onset of freezing usually occurred during late October with the mean

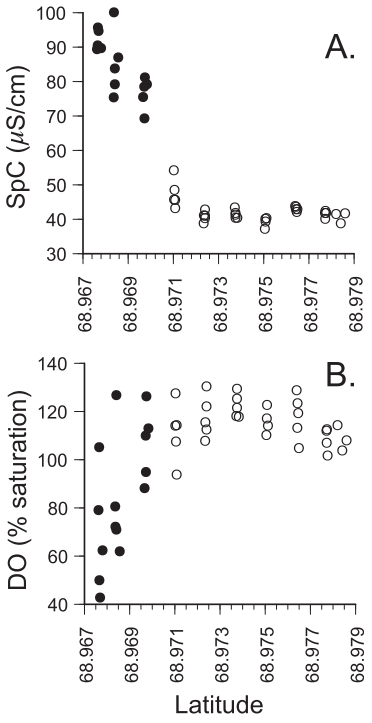

Fig. 2. Specific conductance (SpC, μS cm^{-1}, **A**) and DO (% saturation, **B**) measured in wells at the Kuparuk *aufeis* field as a function of latitude during 12–17 August 2017. Closed circles indicate measurements made in wells (1–15) in the southern portion of the array (wells 1–15); open circles represent wells in the northern portion of the array (16–50).

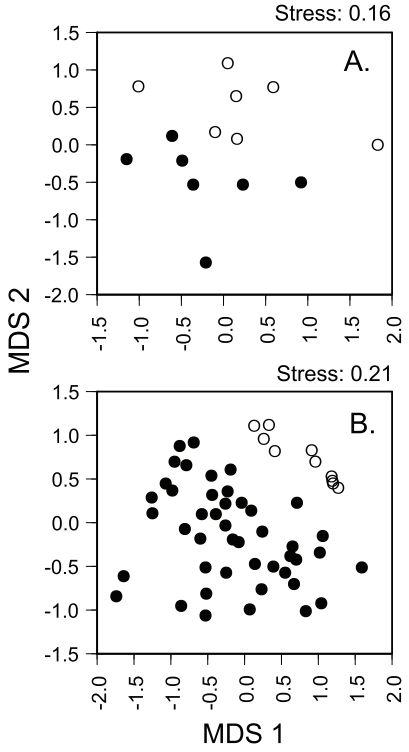

Fig. 3. Nonmetric multidimensional scaling (nMDS) ordination plots of invertebrate assemblage structure based on Bray–Curtis similarities. (**A**) 2-D representation of an nMDS ordination of the numerical abundances of invertebrate taxa sampled from wells during both 14–16 June (open circles) and 12–17 August 2017 (closed circles). ANOSIM indicated that the two clusters were significantly different (Global R = 0.229, sample statistic = 0.018). (**B**) 2-D representation an nMDS ordination of the proportional abundance of invertebrate taxa sampled from surface sediments (open circles) and wells (closed circles) during 12–17 August 2017. ANOSIM indicated that the structure of the invertebrate assemblages of the different habitats was significantly different (Global R = 0.404, sample statistic = 0.001).

ordinal date being 305 ± 2 d (± 1 SE, i.e., 31 October 2016 ± 2 d, range = 12 October to 11 December, excluding one well that apparently froze on 17 February 2017, Table 1). The mean ordinal thaw-date was 184 ± 4 (i.e., 03 July 2017 ± 4 d, range = 28 April to 09 August, Table 1). The mean number of days of well temperatures ≥ 0°C was 115 ± 6 d and mean well temperature during this period was 3.8°C ± 0.1°C (Table 1).

Water chemistry and apparent hydraulic conductivity

During 12–17 August 2017, SpC (μS cm^{-1}) and DO (mg L^{-1}, % saturation) showed strong spatial gradients. SpC measured in the three most southern well transects was higher (84.4 ± 2.3 μS cm^{-1} [N = 15] vs. 42.0 ± 0.6 μS cm^{-1} [N = 31], $p < 0.0001$, two-tailed t-test assuming unequal variance) and DO was lower (10.0 ± 0.8 mg L^{-1} [85.3% ± 6.8% saturation, N = 15] vs. 13.3 ± 0.2 mg L^{-1} [114.9% ± 1.6% saturation, N = 31], $p = 0.001$) than measurements from wells in the seven most northern transects (Table 2, Fig. 2). Similarly, correlation coefficients (r) between July air and well temperatures (when diel extremes are maximized, Table 2) were lower for wells in the three southern transects compared with the seven northern transects (r = 0.138 ± 0.031 [N = 12] vs. 0.266 ± 0.040 [N = 27], $p < 0.02$) and the mean number of days of well temperatures ≥ 0°C were greater for the three southern well transects compared with the northern transects (132 ± 6 d [N = 12] vs. 109 ± 12 d [N = 27], $p < 0.02$). No such pattern was detected ($p > 0.2$) for concentrations of NO_3^-–N (98.9 ± 6.7 μg L^{-1}, range = 46.5–278.0 μg-N L^{-1}, N = 46), NH_4^+–N (4.3 ± 0.2 μg L^{-1}, range = 1.4–15.4 μg L^{-1}, with 75.6 μg L^{-1} as an extreme outlier), SRP (6.3 ± 1.6 μg-P L^{-1}, range = 2.1–7.7 μg-P L^{-1}) and hydraulic conductivity (47.7 ± 8.6 m d^{-1}, N = 38, Table 2). Hydraulic conductivity ranged from 0.1 to 252.5 m d^{-1} (Table 2), with 79% of wells showing rates > 10.0 m d^{-1}, indicating "moderately high (24%)" to "high (55%)" permeability (Bureau of Reclamation 1995). The magnitude of hydraulic conductivity measured in the wells was comparable to that estimated at the field site during winter (i.e., 10s of m d^{-1}) using NMR that enabled estimates at sediment depths up to 10+ m (Terry et al. 2020). Measurements of SpC from surface waters did not differ significantly from wells and showed a similar spatial pattern, with SpC measured from the three southernmost well transects being higher than SpC measured from the northernmost transects (Table 3; ANOVA-GLM, Tukey's LSD, $p < 0.05$). Limited samples from wells during June 2017 indicated no latitudinal gradient of SpC (Table 4; ANOVA-GLM, $p > 0.05$).

Invertebrate abundance and assemblage structure

During 14–16 June 2017, seven exposed wells were sampled. The mean thaw date of these wells was 27 May 2017 (mean ordinal date = 147 ± 9 d [± 1 SE]), indicating that the sediments surrounding them were unfrozen for ~ 19 d prior to sampling. Mean invertebrate abundance in well samples was 242.6 (86.3–450.6, 95% confidence limits; range = 28.5–

Table 3. Summary of surface water chemistry sampled at the locations of surface sediment samples taken during 12–17 Aug 2017 at the Kuparuk *aufeis* field, North Slope, Alaska. Data are shown for all sample locations (N = 10) and samples (S) taken within transects containing wells (W) 1–15 (N = 3) and wells 16–50 (N = 7). Specific conductance was significantly higher within transects containing wells 1–15 than those containing wells 16–15 ($p < 0.05$).

	All samples	S ~W1–15	S ~W16–50
Specific conductance (μS cm^{-1} ± SE)	53.8 ± 5.4	77.2 ± 2.3	43.8 ± 2.3
Dissolved oxygen (mg L^{-1} ± SE)	13.3 ± 0.5	12.9 ± 1.2	13.7 ± 0.5
Dissolved oxygen (% saturation ± SE)	117.4 ± 3.5	113.1 ± 9.1	119.2 ± 3.5
Nitrate-N (μg-N L^{-1} ± SE)	67.6 ± 7.7	80.6 ± 9.0	62.0 ± 10.0
Ammonium-N (μg-N L^{-1} ± SE)	5.2 ± 0.4	5.0 ± 0.7	5.2 ± 0.5
SRP (μg-P L^{-1} ± SE)	4.2 ± 1.3	3.0 ± 0.7	4.8 ± 1.8

Table 4. Summary of chemical attributes of water from wells sampled during 14–16 Jun 2017 at the Kuparuk *aufeis* field, North Slope, Alaska. Data are shown for all wells (N = 7), wells 1–15 (N = 5), and wells 16–50 (N = 2). Specific conductance was not significantly different between wells 1–15 and wells 16–50 ($p > 0.05$).

	All wells	Wells 1–15	Wells 16–50
Specific conductance (μS cm^{-1} ± SE)	61.8 ± 2.4	59.3 ± 1.6	68.2 ± 4.4
Dissolved oxygen (mg L^{-1} ± SE)	9.2 ± 1.1	8.6 ± 1.4	10.6 ± 1.0
Dissolved oxygen (% saturation ± SE)	71.8 ± 8.8	67.9 ± 11.5	81.8 ± 8.8
Nitrate-N (μg-N L^{-1} ± SE)	172.6 ± 38.4	138.4 ± 38.4	258.0 ± 55.2
Ammonium-N (μg-N L^{-1} ± SE)	6.4 ± 0.9	6.9 ± 1.2	5.1 ± 0.2
SRP (μg-P L^{-1} ± SE)	4.8 ± 0.7	5.4 ± 0.8	3.4 ± 0.1

793.7) individuals 10 L^{-1}. Only one well yielded < 30 individuals 10 L^{-1}. Samples from the same wells (N = 7) during August 2017 yielded a mean of 268.7 (27.7–538.2, range = 5.5–978.9) individuals 10 L^{-1}. Major contributors to abundance during June 2017 included the chironomid *Diplocladius cultriger* (44.0% of mean abundance) and the copepod *Attheyella nordenskioldii* (17.9%, Table 5). Mean taxonomic richness during 14–16 June 2017 was 14.0 (10.0–18.3, range = 5–24) taxa 10 L^{-1} $well^{-1}$ with a total of 31 taxa identified (Table 6). Samples from the same wells during August 2017 yielded 30 taxa and a mean richness of 11.1 (7.7–14.9, range = 5–20) taxa 10 L^{-1}. Major contributors to richness during June 2017 included the microcrustacea (8 spp.) and Chironomidae (15 genera). Widespread taxa included the Hydrachnidiae (100% of wells), Nematoda (100%), *A. nordenskioeldii* (86%), *D. cultriger* (71%), Oligochaeta (71%), *Candona* sp. (71%), *Diacyclops languidoides* (57%), *Cletocampus* (57%), *Corynoneura arctica* (57%), and *Hydrobaenus* (57%, Table 6). Mean quantities of organic matter sampled from wells was 0.57 ± 0.21 g AFDM 10 L^{-1} (± 1 SE, range = 0.29–0.46 g 10 L^{-1}). Mean % AFDM was 15.97 ± 5.10% (range = 4.7%–35.6%).

During 12–17 August 2017, invertebrates and organic matter were sampled from 45 wells. Mean invertebrate abundance was 92.4 (45.0–159.3, 95% confidence limits) individuals 10 L^{-1}. Abundance ranged from 1 to 979 individuals 10 L^{-1}; only 8 wells yielded < 10 individuals 10 L^{-1} (Table 5; Fig. 1S). Major contributors included the copepod *A. nordenskioeldii* (16.2% of total mean abundance), the chironomid *Trichotanypus posticalis* (16.2%), the ostracod *Candona* (13.4%), and the Oligochaeta (13.1%) and Nematoda (16.7%). Forty-six taxa were identified (Table 5). Major contributors to richness included the microcrustacea (11 sp.), Chironomidae (17 genera), and the Plecoptera (3 genera). Mean richness was 7.5 (6.2–8.9, range = 1–22) taxa 10 L^{-1} $well^{-1}$. Widespread taxa included *T. posticalis* (73% of wells), *D. languidoides* (58%), *C. arctica* (58%), *A. nordenskioeldii* (49%), *Candona* (49%), and the Nematoda (49%, Table 6). Mean quantity of organic matter was 0.32 ± 0.06 g AFDM 10 L^{-1} $well^{-1}$ (± 1 SE, range = 0.03–1.68 g 10 L^{-1} $well^{-1}$). Mean % AFDM was 10.0 ± 1.5% (range = 2.1%–38.4%).

The mean abundance of invertebrates from surface sediments during 12–17 August 2017 was 952.5 (734.7–1199.8, range = 391–1742) individuals Surber $sample^{-1}$ (i.e., 0.09 m^{-2} of stream bottom). Major contributors included *T. posticalis* (25.2%), *Orthocladius (Orthocladius)* (24.4%), and *Eukiefferiella* (12.3%, Table 5). Forty-two invertebrate taxa were identified (Table 6). Major contributors to richness included the microcrustacea (Cladocera: 1 sp., Copepoda: 3 spp., Ostracoda: 1 sp.), the Chironomidae (18 genera), and the Ephemeroptera (4 genera), Plecoptera (3 genera), and Trichoptera (2 genera). Mean taxonomic richness was 18.6 (13.8–23.3, range = 9–30 taxa) $sample^{-1}$. Widespread taxa included *Baetis* (80% of sample locations), *T. posticalis* (90%), *C. arctica* (90%), *Diamesa* (100%), *Eukiefferiella* (100%), and *O. (Orthocladius)* (100%, Table 6). The mean quantity of organic matter associated with surface sediments was 1.3 ± 0.7 g AFDM $sample^{-1}$ (± 1 SE, range = 0.1–3.9 g $sample^{-1}$). Mean % AFDM was 64.0% ± 10.4% (range = 6.5%–88.6%).

A significant difference in community structure between wells sampled during both 14–16 June and 12–17 August 2017 was detected (N = 7, Fig. 3A; nMDS: 2D stress = 0.16; ANOSIM, Global R = 0.229, sample statistic = 0.018). SIMPER indicated that average Bray–Curtis dissimilarity between wells was 59.3, with 16 taxa collectively contributing ~ 80% (range = 3.5%–6.9%). Among these, *D. cultriger* (6.5% mean total dissimilarity) was present only during June and *Allona excisa* (4.4%) was present only during August (Table 5). The Hydrachnidiae (6.9%), *D. cultriger* (6.5%), and *O.* (*Euorthocladius*) (5.4%) were more abundant during June (two-sample randomization test, $p < 0.05$).

Invertebrate spatial distribution

A significant difference in the proportional abundance of the taxa comprising the invertebrate assemblages for well (N = 45) and surface samples (N = 10) was detected during 12–17 August 2017 (Fig. 3B; nMDS: 2D stress = 0.21; ANOSIM, Global R = 0.404, sample statistic = 0.001). The nMDS plot indicated a wider range of variation of taxonomic assemblage structure for well samples compared with surface samples (Fig. 3B). This observation was supported by multivariate dispersion analysis (MVDISP, Clarke and Gorley 2006) that showed that average rank dissimilarity (RD) of assemblage structure was more than two times higher for wells (RD = 1.025) than surface samples (RD = 0.456). SIMPER indicated that average Bray–Curtis dissimilarity was 78.3, with 22 taxa contributing ~ 80% (range = 1.8%–6.6%). Of these, six taxa occurred only in surface sediments (*Eukiefferiella* [6.6% of mean total dissimilarity], *O.* (*Orthocladius*) [6.0%], *Orthocladius rivularum* [4.9%], *Baetis* [3.7%], *Prosimulium* [2.6%], *Pseudokiefferiella* [1.8%], Table 5) and two taxa occurred only in wells (*D. languidoides* [4.1%], *Acanthocyclops vernalis* [2.1%]). Four others (*Orthocladius* (*Euorthocladius*) [5.2%], *D. cultriger* [2.3%], *Gymnopais* [2.2%], Empididae [1.5%]) showed greater proportional abundance in surface sediments and six (*Candona* [4.4%], *A. nordenskioeldii* [4.1%], Nematoda [4.1%], *Arcynopteryx* [2.0%], *Mesostoma arctica* [2.0%], Capniidae [1.2%]), showed greater proportional abundance in wells (two-sample randomization test, $p < 0.05$). The numerically dominant taxon within the *aufeis* field, *T. posticalis* (5.0% contribution to dissimilarity), showed no significant difference between habitats and contributed substantially to assemblage structure of both surface sediments (29.5% of mean abundance, 13.8%–44.8%, 95% confidence limits) and wells (23.2% [16.0%–30.8%]).

The results of the rarefaction analysis (Fig. 4) indicated that taxonomic richness increased with cumulative abundance following a logarithmic relationship (# taxa for

Table 5. Summary of mean invertebrate abundance from wells (mean # 10 L^{-1} of water sampled [95% CI limits, N = 45]) sampled during 14–16 Jun 2017, and mean invertebrate abundance from wells (mean # 10 L^{-1} of water sampled [95% CI limits, N = 45]) and surface sediments (mean # 0.09 m^{-2} Surber sample [95% CI limits] N = 10) during 12–17 Aug 2017 at the Kuparuk *aufeis* field, North Slope, Alaska.

Major taxon	Family	Genus species	Jun 2017 # 10 L^{-1}	Aug 2017 # 10 L^{-1}	Aug 2017 # 0.09 m^{-2}
Cnidaria	Hydridae	*Hydra*	0.4(0.0–0.9)	0.2(0.0–0.9)	1.9(0.0–5.4)
Turbellaria: Typhoplanida	Typhloplanidae	*Mesostoma arctica*	0.5(0.1–1.1)	1.4(0.4–2.8)	0.8(0.0–2.4)
Turbellaria: Tricladida	—	—	0.4(0.1–0.8)	0.1(0.0–0.3)	0.3(0.0–0.7)
Nematoda	—	—	11.7(2.1–26.7)	15.4(6.0–28.1)	14.8(2.4–33.6)
Oligochaeta	Naididae	*Chaetogaster*	0.0 0.4(0.0–1.1)	12.9(0.0–25.6)	
Oligochaeta	Lumbriculidae	*Rhynchelmis*	0.5(0.1–1.1)	0.5(0.1–1.1)	4.1(0.0–9.8)
Oligochaeta	—	—	20.8(1.6–52.1)	11.2(1.7–31.6)	37.3(1.6–97.2)
Tardigrada	—	—	0.0	<0.1	1.2(0.0–2.8)
Hydrachnidiae	—	—	11.0(4.3–19.6)	0.3(0.1–0.6)	1.6(0.0–4.0)
Collembola	—	—	0.0	0.2(0.0–0.5)	0.0
Ephemeroptera	Baetidae	*Acentrella*	0.0	<0.1	6.0(1.3–11.4)
—	—	*Baetis*	0.0	0.0	20.4(5.4–42.8)
—	Ephemerellidae	*Ephemerella*	0.0	0.0	0.2(0.1–0.5)
—	Heptageniidae	*Cynigmula*	0.0	0.0	4.8(0.0–11.7)
Plecoptera	Capniidae	—	0.1(0.0–0.4)	0.7(0.2–1.4)	0.8(0.0–2.4)
—	Nemouridae	*Nemoura*	0.5(0.0–1.3)	0.5(0.0–1.4)	29.3(0.2–66.8)
—	Perlodidae	*Arcynopteryx*	0.4(0.1–0.7)	0.4(0.2–0.6)	1.9(0.3–4.2)
Trichoptera	Apataniidae	*Apatania*	0.1(0.0–0.4)	<0.1	2.4(0.1–5.4)
—	Brachycentridae	*Brachycentrus*	0.0	0.0	0.1(0.0–0.4)
Diptera	Ceratopogonidae	—	0.0	<0.1	0.0
—	Chironomidae	*Bryophaenocladius*	0.0	<0.1	0.1(0.0–0.3)
—	—	*Cladotanytarsus*	0.0	<0.1	0.0
—	—	*Conchapelopia*	0.0	<0.1	0.0
—	—	*Constempellina*	0.1(0.0–0.4)	0.2(0.0–0.9)	0.0
—	—	*Corynoneura arctica*	5.7(0.5–15.0)	4.7(1.7–9.0)	36.5(23.3–49.4)
—	—	*Diamesa*	0.1(0.0–0.4)	0.1(0.0–0.3)	43.6(23.1–68.9)
—	—	*Diplocladius cultriger*	107.9(1.2–309.4)	<0.1	19.5(2.4–40.0)
—	—	*Eukiefferiella*	0.7(0.0–1.6)	<0.1	117.4(56.8–181.1)
—	—	*Heterotrissocladius*	0.3(0.0–0.5)	0.2(0.0–0.4)	1.7(0.0–4.8)
—	—	*Hydrobaenus*	1.4(0.3–2.9)	1.6(0.6–2.9)	11.5(3.2–20.4)
—	—	*Krenosmittia halvorseni*	3.8(0.0–8.8)	0.4(0.0–1.2)	0.0
—	—	*Limnophyes*	0.1(0.0–0.4)	0.1(0.0–0.4)	0.0
—	—	*Orthocladius (Orthocladius)*	0.0	0.0	84.1(25.4–162.3)
—	—	*O. (Euorthocladius)*	6.1(2.0–12.0)	0.8(0.2–1.5)	72.5(39.3–105.6)
—	—	*Paracricotopus*	0.0	<0.1	0.0
—	—	*Paralimnophyes*	0.0	<0.1	0.0
—	—	*Pseudodiamesa*	0.0	0.1(0.0–0.2)	6.2(1.2–12.1)
—	—	*Pseudokiefferiella*	0.0	0.0	18.4(0.0–44.4)
—	—	*Rheotanytarsus*	0.0	0.0	3.2(0.0–9.6)
—	—	*Trichotanypus posticalis*	3.0(0.0–8.4)	14.9(7.1–25.2)	240.8(108.7–375.0)
—	—	*Tvetenia*	0.0	0.0	2.6(0.0–5.7)
—	Empididae	—	0.0	0.0	5.6(0.8–12.8)
—	Psychodidae	*Psychoda*	0.0	0.0	0.9(0.0–2.5)
—	Simuliidae	*Gymnopais*	0.3(0.0–0.8)	<0.1	8.4(0.3–16.8)
—	—	*Prosimulium*	0.0	0.0	5.9(3.2–9.0)

(Continues)

Table 5. Continued

Major taxon	Family	Genus species	Jun 2017 # 10 L^{-1}	Aug 2017 # 10 L^{-1}	Aug 2017 # 0.09 m^{-2}
—	Tipulidae	*Antocha*	0.0	0.0	0.1(0.0–0.3)
—	—	*Dicranota*	0.0	<0.1	1.7(0.0–4.1)
Ostracoda	Candonidae	*Candona*	3.9(1.4–6.4)	12.6(3.0–26.8)	31.8(2.4–71.2)
Cladocera	Chydoridae	*Acroperus harpae*	0.0	0.1(0.1–0.6)	0.8(0.0–2.4)
—	—	*Alonella exilis*	0.0	0.7(0.0–1.5)	0.0
—	—	*Chydorus sphaericus*	0.1(0.0–0.4)	0.6(0.1–1.1)	0.0
—	—	*Eurycercus glacialis*	0.4(0.0–1.2)	0.3(0.0–0.6)	0.0
—	Daphniidae	*Daphnia middendorffiana*	0.0	<0.1	0.0
Copepoda	Cyclopidae	*Acanthocyclops vernalis*	1.7(0.0–4.3)	2.1(0.6–4.7)	0.0
—	—	*Diacyclops languidoides*	4.3(0.5–10.8)	5.4(1.8–10.0)	0.0
—	—	*Eucyclops agilis*	0.0	0.1(0.0–0.3)	0.0
—	Harpacticoida	*Attheyella nordenskioeldii*	42.1(8.7–91.4)	15.1(2.7–34.1)	18.4(0.0–43.2)
—	—	*Cletocampus*	12.9(1.1–32.0)	0.4(0.0–1.0)	2.3(0.0–7.2)
—	—	*Moraria*	0.1(0.0–0.4)	0.0	0.0

wells = $10.729 \pm 0.152 \times \ln$ [individuals] – 40.464 ± 1.139, ± 95% confidence limits, $R^2 = 0.998$, $p < 0.0001$; # taxa for surface sediments = $10.828 \pm 0.527 \times \ln$ [individuals] – 55.484 ± 4.429, $R^2 = 0.996$, $p < 0.001$). The slopes of the equations did not differ significantly (ANCOVA-GLM, $p = 0.658$). For a given accumulated abundance, however, richness was higher (~ 15 taxa) for wells than surface sediments (ANCOVA-GLM, $p < 0.0001$, Fig. 4). The rarefaction curves did not achieve asymptotes and so did not allow robust estimates of richness. Total taxonomic richness indicated by these analyses, however, was 49 ± 5 taxa for 45 samples from wells and 43 ± 7 taxa for 10 samples from surface sediments. Although more samples were taken from wells than surface sediments, fewer individuals were accumulated from wells than surface sediments (4229 vs. 9485 individuals).

Following the detection of SpC and DO concentration gradients within the well array (Fig. 2), we predicted that the invertebrate fauna would show a corresponding spatial pattern. This was hypothesized to be due to a stronger link to deep groundwater habitat in the southern portion of the array (potentially contributing to high SpC, low DO; *see* the Discussion section). Our analyses revealed differences in assemblage structure between high SpC ($N = 15$) and low SpC wells ($N = 30$) during 12–17 August 2017 (Fig. 5; nMDS: 2D stress = 0.20; ANOSIM, Global R = 0.261, sample statistic = 0.001). SIMPER indicated that average Bray–Curtis dissimilarity was 71.2 with 14 taxa contributing ~ 80% (range = 2.6%–10.3%). Of these, the abundances of *A. nordenskioeldii* (8.6% of mean total dissimilarity, 40.6 [4.0–86.6, 95% confidence limits] individuals 10 L^{-1} from high SpC wells vs. 2.2 [0.9–3.7] individuals 10 L^{-1} in low SpC wells), Nematoda (8.4%, 32.4 [8.1–63.5] vs. 6.8 [1.3–14.1] individuals 10 L^{-1} $well^{-1}$), Turbellaria: Tricladida (7.3%, 0.4 [0.1–0.9] vs. 0.0 individuals 10 L^{-1} $well^{-1}$), *M. arctica* (6.2%, 3.4 [0.9–6.5] vs. 0.4 [0.0–1.0] individuals 10 L^{-1} $well^{-1}$), Oligochaeta (5.8%, 30.9 [2.7–78.7] vs. 1.6 [0.6–2.8] individuals 10 L^{-1} $well^{-1}$), Capniidae (3.0%, 1.9 [0.5–3.6] vs. 0.1 [0.0–0.3] individuals 10 L^{-1} $well^{-1}$), and *Alonella exilis* (2.3%, 2.0 [0.1–4.2] vs. 0.0 individuals 10 L^{-1} $well^{-1}$) were significantly greater in high compared with low SpC wells (two-sample randomization test, $p < 0.05$). Conversely, the abundance of *T. posticalis* was significantly greater in low compared with high SpC wells (10.3%, 6.0 [0.6–15.0] individuals 10 L^{-1} of water from high SpC wells vs. 19.3 [9.0–34.8] individuals 10 L^{-1} from low SpC wells, two-sample randomization test, $p < 0.05$).

Discussion

The Kuparuk *aufeis* field provides subsurface habitat for a rich assemblage of freshwater invertebrates (49 ± 5 taxa estimated using rarefaction, $\bar{X}$ ± 95% CI) that is distinct from that occurring in surface habitats. This subsurface assemblage is also spatially extensive, being detected in wells at a mean depth of ~ 69 cm throughout the entire ~ 40-ha well array (Fig. 1S). This level of richness is presumably enabled by the relatively high porosity of the subsurface sediments combined with a high level of connectivity between pore spaces (Strayer et al. 1997), as indicated by high hydraulic conductivity magnitudes measured both directly within the wells (~ 1 m deep) using NaCl as a tracer and indirectly at greater depths (> 10 m deep) using NMR (Terry et al. 2020). To our knowledge, this is the first demonstration of a groundwater (e.g., hyporheic/parafluvial/groundwater) invertebrate fauna in a region of continuous permafrost.

Table 6. Summary of % samples in which different invertebrate taxa were present during 14–16 Jun 2017 (N = 7 wells) and 12–17 Aug 2017 (N = 45 wells, N = 10 surface sediment samples) from the Kuparuk *aufeis* field, North Slope, Alaska.

Major taxon	Family	Genus species	Jun 2017 % wells	Aug 2017 % wells	Aug 2017 % samples
Cnidaria	Hydridae	*Hydra*	28.6	4.4	20.0
Turbellaria: Typhoplanida	Typhloplanidae	*Mesostoma arctica*	42.9	31.1	10.0
Turbellaria: Tricladida	—	—	42.9	8.9	20.0
Nematoda	—	—	100.0	48.9	40.0
Oligochaeta	Naididae	*Chaetogaster*	0.0	6.7	30.0
—	Lumbriculidae	*Rhynchelmis*	42.9	17.8	30.
—	—	—	57.1	42.2	40.0
Tardigrada	—	—	0.0	4.4	20.0
Hydrachnidiae	—	—	100.0	13.3	20.0
Collembola	—	—	0.0	13.3	0.0
Ephemeroptera	Baetidae	*Acentrella*	0.0	2.2	60.0
—	—	*Baetis*	0.0	0.0	80.0
—	Ephemerellidae	*Ephemerella*	0.0	0.0	30.0
—	Heptageniidae	*Cynigmula*	0.0	0.0	30.0
Plecoptera	Capniidae	—	14.3	22.2	10.0
—	Nemouridae	*Nemoura*	11.1	11.1	40.0
—	Perlodidae	*Arcynopteryx*	28.6	4.4	40.0
Trichoptera	Apataniidae	*Apatania*	14.3	2.2	40.0
—	Brachycentridae	*Brachycentrus*	0.0	0.0	20.0
Diptera	Ceratopogonidae	—	0.0	2.2	0.0
—	Chironomidae	*Bryophaenocladius*	0.0	2.2	10.0
—	—	*Cladotanytarsus*	0.0	2.2	0.0
—	—	*Conchapelopia*	0.0	4.4	0.0
—	—	*Constempellina*	14.3	4.4	0.0
—	—	*Corynoneura arctica*	57.1	57.8	90.0
—	—	*Diamesa*	14.3	4.4	100.0
—	—	*Diplocladius cultriger*	71.4	2.2	50.0
—	—	*Eukiefferiella*	28.6	2.2	100.0
—	—	*Heterotrissocladius*	28.6	11.1	10.0
—	—	*Hydrobaenus*	57.1	31.1	50.0
—	—	*Krenosmittia halvorseni*	42.9	6.7	0.0
—	—	*Limnophyes*	14.3	6.7	0.0
—	—	*Orthocladius (Orthocladius)*	0.0	0.0	100.0
—	—	*O. (Euorthocladius)*	85.7	24.4	100.0
—	—	*Paracricotopus*	0.0	2.2	0.0
—	—	*Paralimnophyes*	0.0	2.2	0.0
—	—	*Pseudodiamesa*	0.0	6.7	50.0
—	—	*Pseudokiefferiella*	0.0	0.0	30.0
—	—	*Rheotanytarsus*	0.0	0.0	10.0
—	—	*Trichotanypus posticalis*	28.6	73.3	90.0
—	—	Tvetenia	0.0	0.0	30.0
—	Empididae	—	0.0	0.0	40.0
—	Psychodidae	*Psychoda*	0.0	0.0	20.0
—	Simuliidae	*Gymnopais*	14.3	2.2	40.0
—	—	*Prosimulium*	0.0	0.0	90.0
—	Tipulidae	*Antocha*	0.0	0.0	10.0
Diptera	—	*Dicranota*	0.0	2.2	30.0

(Continues)

Table 6. Continued

Major taxon	Family	Genus species	Jun 2017 % wells	Aug 2017 % wells	Aug 2017 % samples
Ostracoda	Candonidae	*Candona*	71.4	40.0	40.0
Cladocera	Chydoridae	*Acroperus harpae*	0.0	2.2	10.0
—	—	*Alonella exilis*	0.0	8.9	0.0
—	—	*Chydorus sphaericus*	14.3	13.3	0.0
—	—	*Eurycercus glacialis*	14.3	11.1	0.0
—	Daphniidae	*Daphnia middendorffiana*	0.0	2.2	0.0
Copepoda	Cyclopidae	*Acanthocyclops vernalis*	28.6	33.3	0.0
—	—	*D. languidoides*	57.1	57.8	0.0
—	—	*Eucyclops agilis*	0.0	4.4	0.0
—	Harpacticoida	*Attheyella nordenskioeldii*	85.7	48.9	30.0
—	—	*Cletocampus*	57.1	8.9	10.0
—	—	*Moraria*	14.3	0.0	0.0

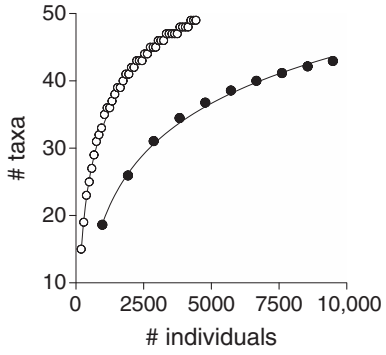

Fig. 4. Rarefaction curves for invertebrates sampled from wells (closed circles) and surface sediments (open circles). The mean cumulative number of taxa per number of samples is plotted as a function of accumulated number of individuals sampled. Accumulated number of individuals was calculated on an accumulated sample basis, following Gotelli and Colwell (2011), see the Methods section. The increase in taxonomic richness per individual follows a logarithmic relationship (# taxa for wells = 10.729 × ln [accumulated individuals] − 40.464, R^2 = 0.998, $p < 0.001$; # taxa for surface sediments = 10.828 × ln [accumulated individuals] − 55.484, R^2 = 0.996, $p < 0.001$). To simplify presentation the mean abundance and taxon number of $N = 1$ well samples (96.5 individuals, 15 taxa) is not shown.

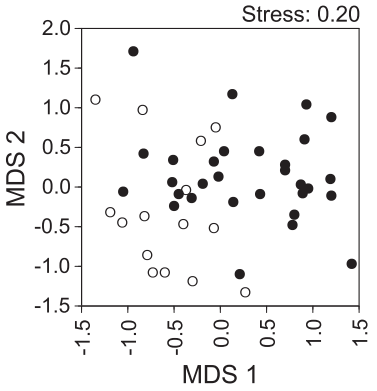

Fig. 5. Two-dimensional representation of a nonmetric multidimensional scaling (nMDS) ordination of the numerical abundances of invertebrate taxa sampled from wells (1–15, open circles) with relatively high levels of specific conductance (SpC, μS cm^{-1}, i.e., Fig. 1) and wells with relatively low levels of SpC (16–50, closed circles). ANOSIM indicated that the structure of the invertebrate assemblages sampled from the different well types were significantly different (Global R = 0.261, sample statistic = 0.001).

We initially predicted that an unfrozen, water-saturated layer of sediments would exist directly beneath the surficial ice layer of the *aufeis* during winter (Terry et al. 2020). Instead, we found an unfrozen layer ~ 3 to 5 m below the sediment-ice interface (Terry et al. 2020). Consequently, our wells (< 1 m depth) sampled seasonally rather than perennially unfrozen habitat. Nevertheless, sampling revealed a relatively rich subsurface fauna (31 taxa, Table 5) only ~ 19 d after thawing (14–16 June 2017). Although freeze tolerance has been documented for some freshwater arctic invertebrates (Lencioni 2004), it is likely that the habitat surrounding recently thawed wells was colonized by migrants from the deeper, perennially unfrozen sediments in the southern portion of the well array (Terry et al. 2020; also *see* the Groundwater upwelling drives spatial patterns of subsurface invertebrate distributions section below).

Surface and subsurface invertebrate assemblages are distinct

The number of invertebrate taxa from well (49 ± 5 taxa, $\bar{X}$ ± 95% CI) and surface habitats (43 ± 7 taxa) during 12–17 August 2017 was at statistical parity, which was surprising given the lower richness in subsurface habitats in large, riverine gravel-aquifer systems elsewhere (Stanford et al. 1994; Ward and Voelz 1994). Although the rarefaction curves did

not attain asymptotes for either habitat, the majority of total taxon richness was presumably represented in the samples. For example, a total of 64 taxa was detected from replicated surface-sediment samples taken annually for more than a decade (2001–2012) from a reach of the upper Kuparuk River ~ 40 km upstream of the *aufeis* field during 2001 to 2012 (Kendrick et al. 2019). Given that surface and subsurface samples yielded a large fraction of the likely possible taxa in this river system (i.e., ~ 64 as documented by Kendrick et al. 2019), we have some confidence in concluding that richness between these habitats is probably not fundamentally different.

Comparisons of taxonomic richness between well and surface habitats should be assessed with caution due to differences in sampling methods and physical context (*see* the Methods: Statistical analysis of temporal and spatial patterns of invertebrate assemblages section above). Nevertheless, rarefaction analysis indicated that wells yielded a consistently higher level of richness (e.g., ~ 15 taxa) for a given cumulative abundance within the range of data overlap (~ 1000–4500 individuals, Fig. 4). This may be explained by higher heterogeneity of subsurface habitats (e.g., upwelling and downwelling zones), that likely contributed to higher species turnover among habitat patches compared with surface sediments. This is supported by nMDS analyses indicating a wider range of variation of taxonomic assemblage structure among well samples compared with surface sediments (Fig. 3B). Evidence suggesting significant heterogeneity of subsurface habitats is also found in the latitudinal gradient of SpC and DO concentrations (cf. Figs. 2 and 5).

Although the taxonomic richness of the invertebrate assemblages documented at the Kuparuk *aufeis* field was similar between subsurface and surface habitats, nMDS analysis indicated significant differences in assemblage structure. The Crustacea, for example, were major contributors to richness only for subsurface habitats (11 taxa [22%] from wells vs. 4 [9%] taxa from surface sediments). At a finer taxonomic level, two categories of taxa occurring within the *aufeis* field were recognized: taxa occurring only in subsurface habitats and those occurring in both subsurface and surface habitats. The cyclopoid copepods *D. languidoides* and *A. vernalis*, and the chironomid midge *Krenosmittia halvorseni* occurred only in subsurface habitats. In the Arctic, *D. languidoides* and *A. vernalis* have been documented from tundra pools in Alaska (Reed 1962; Tash 1971; Reid et al. 1991) and Siberia (Fefilova et al. 2008, 2013). These taxa, however, have also been documented from groundwater habitats in temperate North America in physical contexts similar to that documented at the Kuparuk *aufeis* field (i.e., river-associated, perennially unfrozen, gravel aquifers, Reid et al. 1991, Ward and Voelz 1994). *Diacyclops* is a large genus with numerous groundwater specialists, including prominent members of subsurface riverine invertebrate assemblages (e.g., *D. languidoides*, Ward and Voelz 1990, 1994; Williams 1993, Stanford et al. 1994). Similarly, permanent groundwater-dwelling populations of *A. vernalis* have been documented (Ward and Voelz 1990, 1994; Reid and Strayer 1994; Stanford et al. 1994). Finally, species of the genus *Krenosmittia* are hyporheic specialists that complete larval development in subsurface habitats (Ferrington 1984; Ward and Voelz 1990).

Although most invertebrate taxa documented in this study occurred, to varying degrees, in both surface and subsurface habitats, some were well represented in both habitats. The chironomid midge *T. posticalis* provides an excellent example. At the Kuparuk *aufeis* field, *T. posticalis* was a major component of the surface assemblage, where it comprised ~ 30% of invertebrate abundance, and of the subsurface assemblage where it comprised ~ 23% of abundance. Although differences in sampling approach do not allow direct comparisons of abundance between habitats, no significant difference between proportional contributions of *T. posticalis* to assemblage structure were detected, indicating that this taxon is a significant contributor to assemblage structure in all three physical dimensions of the *aufeis* field.

Groundwater upwelling drives spatial patterns of subsurface invertebrate distributions

The detection of a latitudinal gradient in SpC (decreasing from S to N) and DO (increasing from S to N) concentrations (Fig. 2), in combination with a parallel gradient in the strength of correlation between subsurface water temperatures and air temperatures (increasing from S to N), indicate the potential for widespread groundwater upwelling in the southern portion of the well array. Elevated SpC and reduced DO concentrations have been widely used as indicators of groundwater, with elevated SpC attributed to long periods of contact with mineral substrata and reduced DO concentrations attributed to biological uptake and limited reaeration in subsurface flowpaths (Fraser and Williams 1998; Alexander and Caissie 2003). Compared with the SpC of the mainstem Kuparuk River in the vicinity of the *aufeis* field (~ 49–56 μS cm^{-1}, McNamara et al. 2008), the SpC of well water in the southern three well transects ranged from ~ 75 to 100 μS cm^{-1} while the SpC from the northern six transects ranged from ~ 37 to 44 μS cm^{-1}. These differences indicate that the subsurface water in the southern portion of the well array (~ 9 ha of the ~ 40-ha well array) had a source distinct from surface water and is likely groundwater rather than hyporheic flow (Fraser and Williams 1998; Alexander and Caissie 2003). The relatively high independence of diel fluctuations of air and subsurface water temperature, as found in the southern portion of the well array, has also been previously used to identify zones of hyporheic and groundwater flow (Evans and Petts 1997; Alexander and Caissie 2003; Hannah et al. 2009).

In addition to indicating widespread upwelling in the southern portion of the well array, spatial patterns of DO concentrations and temperature provided evidence for widespread (~ 31 ha) downwelling in the northern portion. During

August 2017, DO concentrations in essentially all wells of the seven northern-most transects were above saturation (Fig. 2). This spatial pattern is likely due to downwelling surface water that was saturated with DO due to photosynthesis by dense mats of bryophytes and filamentous algae in surface channels (A. D. Huryn, pers. obs.; M. N. Gooseff, pers. obs.). Following downwelling, high DO levels were presumably maintained by low biological DO uptake due to low amounts of organic matter in the subsurface sediments. Our detection of groundwater upwelling in the southern portion of the well array and surface water downwelling in the northern portion follows Terry et al. (2020), who detected a zone of deep *talik* in the southern portion of the well array.

Differences in invertebrate assemblage structure and abundance between upwelling (higher richness and abundance) and downwelling (lower richness and abundance) zones have been previously shown for gravel-bed rivers (Stanley and Boulton 1993; Malard et al. 2003). Such differences have been attributed to greater representation of hyporheic and groundwater specialists in upwelling zones (Malard et al. 2003). Similarly, we found significantly different assemblage structures in upwelling and downwelling zones of the Kuparuk *aufeis* field. Specific taxa contributing to these differences included the turbellarian *M. arctica*, the harpacticoid copepod *A. nordenskioeldii*, and larvae of the stonefly family Capniidae. Each of these showed significantly higher abundances in wells within the upwelling zone. *A. nordenskioeldii* has been previously reported from tundra ponds in arctic Alaska (Reed 1962). Williams (1993), however, reported this taxon from subsurface habitats in Ontario, Canada, and concluded that it was a hyporheic specialist there. Similarly, the Capniidae contains hyporheic specialists (Stanford and Gaufin 1974, Stanford et al. 1994, see below). Only one taxon, the midge *T. posticalis*, showed significantly higher abundances in wells in the downwelling zone. Given the generally abundant distribution of *T. posticalis* in all three spatial dimensions of the *aufeis* field, we assume that downwelling water into the relatively porous sediments results in efficient colonization of subsurface habitats, rather than specific adaptations per se.

Evidence for widespread groundwater habitats associated with *aufeis* fields in the Arctic

Evidence for the existence of a more widespread subsurface fauna in arctic Alaska is provided by several stonefly species. Nine of the 25 stonefly species reported from the North Slope of Alaska, for example, are members of a specialized hyporheic fauna that is associated with *aufeis* (Kendrick and Huryn 2014). Although apparently not present at the Kuparuk River *aufeis* field, *Paraperla frontalis* (Plecoptera: Chloroperlidae) and several species of *Isocapnia* (i.e., *I. crinita*, *I. grandis*, *I. integra* [Plecoptera: Capniidae]), all groundwater/hyporheic specialists (Stanford and Gaufin 1974; Stanford et al. 1994), have been documented from *aufeis* fields in arctic Alaska (e.g., Saviukviak River *aufeis* field, Ribdon River *aufeis* field, Ivishak River *aufeis* field, Kendrick and Huryn 2014, A. D. Huryn, pers. obs.; Fig. 6). The life cycles of *P. frontalis* and species of *Isoperla* begin when eggs deposited in the river channel are entrained into subsurface habitats where larval development takes place. Several years later, mature larvae return to the stream channel to emerge as adults. Both taxa have been collected from wells up to 3 km from the main channels of alluvial rivers in the Flathead River valley of Montana (Stanford et al. 1994), and their presence in Alaska indicates that *aufeis*-maintained habitats may be remarkably similar to hyporheic habitats of some temperate river-floodplain ecosystems. Stanford et al. (1994), in fact, predicted that subsurface "assemblages similar to those in the Flathead River valley likely exist in many well-oxygenated interstitial aquifers fed by river interflow in North America and elsewhere, depending on the origin and attributes of the porous milieu." The occurrence of these same taxa in association with *aufeis* fields on the North Slope of Alaska indicates that localized populations of groundwater fauna may be relatively widespread in spring stream-*aufeis* ecosystems elsewhere in the Arctic.

Fig. 6. Adult males (small, dark individuals on left), a female (center), and six molted larval exoskeletons of *Isocapnia integra* (Plecoptera: Capniidae) on an *aufeis*. Larvae completed their life cycles deep within the sediments beneath the *aufeis* (Ivishak River, North Slope, Alaska, A. D. Huryn, 19 June 2017).

Ecological significance of *aufeis* fields

Although the physical hydrology of *aufeis* has received substantial attention (Yoshikawa et al. 2007; Alekseyev 2015) little is known about their ecology, even though they have been predicted to have significant effects on stream ecosystems. For example, it has been suggested that *aufeis* function as "oases" during summer by providing meltwater to downstream habitats otherwise dependent on seasonal precipitation and

thawing of the active layer (Kane and Slaughter 1972; Sokolov 1991; Li et al. 1997), provide seasonal habitat for fishes (Sandstrom 1995) and mammals (Gill and Kershaw 1981), and provide a form of disturbance that maintains characteristic plant communities (Alekseyev 2015). Prior to the present study, little was known about the potentially enormous subsurface habitat in the form of perennially unfrozen sediments maintained by *aufeis*, and a subsurface, freshwater fauna was unanticipated for the Arctic due to the assumption of continuous permafrost beneath seasonally thawed, hyporheic sediments surrounding stream beds (Edwardson et al. 2003; Brosten et al. 2006; Zarnetske et al. 2008). The presence of expansive aquifers, containing a rich biotic community, that are interconnected with surface habitats, however, indicates that river ecosystems affected by *aufeis* fields are more complex than formerly perceived and are likely to be high-latitude, ecological analogues of temperate gravel-bed rivers with similar physical structure and highly bioreactive aquifers (Stanford et al. 1994). At minimum, the potentially extensive interaction zone between river and aquifer and the flux of water and particulate and dissolved carbon and organisms between these compartments requires a more complex conceptual model of river-floodplain ecosystem structure and function than is currently acknowledged for the Arctic (Huryn 2021). Finally, the role of *aufeis* in associated ecosystems within the next century, although poorly understood at present, is likely to be in a state of flux due to climate change, particularly in the Arctic where temperatures are rising rapidly due to polar amplification of greenhouse warming (Chapin et al. 2006; Martin et al. 2009; Overland et al. 2015). Although major *aufeis* will continue to form during winter, even given predictions of anticipated winter warming (Cherry et al. 2014; Overland et al. 2015), the persistence of ice during the summer thaw will likely decline (Pavelsky and Zarnetske 2017), which will affect the seasonality of flow of receiving aquifers, streams, and rivers. Perhaps more significant is the effect of climate change on patterns of precipitation required to recharge the aquifers of springs forming *aufeis*. The source of water recharging these aquifers on the North Slope of Alaska is not well understood (Hall and Roswell 1981; Yoshikawa et al. 2007; Kane et al. 2013), but it is likely that the associated spring-*aufeis* systems will show a range of hydrological responses ranging from "transient" (local aquifer is depleted and *aufeis* fails to form) to "stable" (aquifer is maintained, Cartwright et al. 2020), depending on recharge dynamics. Nevertheless, under scenarios that include warming and increased summer drying for the Arctic (ACIA 2005; Chapin et al. 2006), multiple emerging roles for the groundwater communities maintained by *aufeis* can be envisioned, including their potential as sources of colonizers in the event perennially saturated, interstitial habitat become more widespread due to winter warming (Huryn et al. 2005), and the potential for stable *aufeis*-spring ecosystems to function as refuges in the event of widespread summer drying.

References

ACIA. 2005. Arctic climate impact assessment. Cambridge: Cambridge Univ. Press.

Alekseyev, V. R. 2015. Cryogenesis and geodynamics of icing valleys. Geodyn. Tectonophys. **6**: 171–224.

Alexander, M. D., and D. Caissie. 2003. Variability and comparison of hyporheic water temperatures and seepage fluxes in a small Atlantic salmon stream. Ground Water **41**: 72–82.

Anderson, T., P. S. Cranston, and J. H. Epler [eds.]. 2013. The larvae of Chironomidae (Diptera) of the Holarctic region: Keys and diagnoses—Larvae. Insect Syst Evol Suppl. **66**: 1–571.

Benke, A. C., and A. D. Huryn. 2006. Secondary production of macroinvertebrates, pp. 691–710. *In* F. R. Hauer and G. A. Lamberti [eds.], Methods in Stream Ecology, 2nd Edition. San Diego: Academic Press.

Boulton, A. J., M.-J. Dole-Olivier, and P. Marmonier. 2004. Effects of sample volume and taxonomic resolution on assessment of hyporheic assemblage composition sampled using a Bou-Rouch pump. Arch. Hydrobiol. **159**: 327–355.

Boulton, A. J., T. Datry, T. Kasahara, M. Mutz, and J. A. Stanford. 2010. Ecology and management of the hyporheic zone: Stream-groundwater interactions of running waters and their floodplains. J. N. Am. Benthol. Soc. **29**: 26–40.

Bowden, W. B., and others. 2014. Ecology of streams of the Toolik region, p. 173–237. *In* J. E. Hobbie and G. W. Kling [eds.], Alaska's changing Arctic: Ecological consequences for tundra, streams and lakes. New York, NY: Oxford Univ. Press.

Brosten, T. R., J. H. Bradford, J. P. McNamara, J. P. Zarnetske, M. N. Gooseff, and W. B. Bowden. 2006. Profiles of temporal thaw depths beneath two arctic stream types using ground-penetrating radar. Permafr. Periglac. Process. **17**: 341–355.

Brown, J., O. J. Ferrians, Jr., J. A. Heginbottom and E. S. Melnikov. 1997. Circum-Arctic map of permafrost and ground-ice conditions. Circum-Pacific Map Series MAP CP-45. U.S. Department of the Interior, U.S. Geological Survey.

Cartwright, J. M., and others. 2020. Oases of the future? Springs as potential hydrologic refugia in drying climates. Front. Ecol. Environ. **18**: 245–253.

Chapin, F. S., III, and others. 2006. Building resilience and adaptation to manage arctic change. Ambio **35**: 198–202.

Cherry, J. E., S. J. Déry, Y. Cheng, M. Stieglitz, A. S. Jacobs, and F. Pan. 2014. Climate and hydrometeorology of the Toolik Lake region and the Kuparuk River basin: Past, present, and future, p. 21–60. *In* J. E. Hobbie and G. W. Kling [eds.], Alaska's changing Arctic: Ecological consequences for tundra, streams and lakes. New York, NY: Oxford Univ. Press.

Childers, J. M., C. E. Sloan, J. P. Meckel, and J. W. Nauman. 1977. Hydrologic reconnaissance of the eastern North Slope, Alaska, 1975 (No. 77-492). US Geological Survey.

Clark, I. D., and B. Lauriol. 1997. Aufeis of the Firth River basin, Northern Yukon, Canada: Insights into permafrost hydrology and karst. Arct. Alp. Res. **29**: 240–252.

Clarke, K. R., and R. N. Gorley. 2006. Primer V6. User Manual/ Tutorial. PRIMER-E, Plymouth, UK.

Collett, T. S., K. J. Bird, K. A. Kvenvolden, and L. B. Magoon. 1989. Map showing the depth to the base of the deepest ice-bearing permafrost as determined from well logs, North Slope, Alaska (Map OM-222). Department of the Interior, U.S. Geological Survey, Oil and Gas Investigations.

Craig, P. C., and P. J. McCart. 1975. Classification of stream types in Beaufort Sea drainages between Prudhoe Bay, Alaska, and the Mackenzie delta, NWT, Canada. Arct. Alp. Res. **7**: 183–198.

Day, R. W., and G. P. Quinn. 1989. Comparisons of treatments after an analysis of variance in ecology. Ecol. Monogr. **59**: 433–463.

Edwardson, K. J., W. B. Bowden, C. Dahm, and J. Morrice. 2003. The hydraulic characteristics and geochemistry of hyporheic and parafluvial zones in arctic tundra streams, North Slope, Alaska. Adv. Water Resour. **26**: 907–923.

Evans, E. C., and G. E. Petts. 1997. Hyporheic temperature patterns within riffles. Hydrol. Sci. J. **42**: 199–213.

Fefilova, E. B., O. A. Loskutova, and S. V. Pestov. 2008. Microbenthic crustacean communities in tundra lakes of northeast European Russia. Aquat. Ecol. **42**: 449–461.

Fefilova, E. B., O. Dubovskaya, O. Kononova, and L. Khokhlova. 2013. A comparative study of the freshwater copepods of two different regions of the central Palaearctic: European and Siberian. J. Nat. Hist. **47**: 805–819.

Ferrington, L. C. 1984. Evidence for the hyporheic zone as a microhabitat of *Krenosmittia* spp. larvae (Diptera: Chironomidae). J. Freshwater Ecol. **2**: 353–358.

Fraser, B. G., and D. D. Williams. 1998. Seasonal boundary dynamics of a groundwater/surface-water ecotone. Ecology **79**: 2019–2031.

Gill, D., and G. P. Kershaw. 1981. Ecological role of river icings in the Tsichu River valley, Northwest Territories, Canada. IAHS **131**: 119–125.

Gooseff, M., and A. D. Huryn. 2019. Effects of aufeis on the structure and function of Arctic river-floodplain ecosystems, Alaska. 2016-2017. Arctic Data Cente. https://doi.org/10.18739/A20P0WR15

Gotelli, N. J., and R. K. Colwell. 2011. Estimating species richness, p. 39–54. *In* A. E. Magurran and B. J. McGill [eds.], Biological diversity: Frontiers in measurement and assessment. New York, NY: Oxford Univ. Press.

Hall, D. K. 1979. Geomorphic processes on the North Slope of Alaska. *In* NASA technical memorandum TM 79720. Greenbelt, MD: Goddard Space Flight Center.

Hall, D. K. 1980. Mineral precipitation in North Slope river icings. Arctic **33**: 343–348.

Hall, D. K., and C. Roswell. 1981. The origin of water feeding icings on the eastern North Slope of Alaska. Polar Rec. **20**: 433–438.

Hannah, D. M., I. A. Malcolm, and C. Bradley. 2009. Seasonal hyporheic temperature dynamics over riffle bedforms. Hydrol. Process. **23**: 2178–2194.

Hamilton, T. D. 1978. Surficial geologic map of the Philip Smith Mountains quadrangle, Alaska. U.S. Geological Survey Miscellaneous Field Studies Map MF-879-A, 1: 250,000.

Huryn, A. D., K. A. Slavik, R. L. Lowe, S. M. Parker, D. S. Anderson, and B. J. Peterson. 2005. Landscape heterogeneity and the biodiversity of Arctic stream communities: A habitat template analysis. Can. J. Fish. Aquat. Sci. **62**: 1905–1919.

Huryn, A. D. 2021. Ecology of arctic streams & rivers, p. 181–218. *In* D. N. Thomas [ed.], Arctic ecology. London, UK: Wiley-Blackwell.

Kane, D. L., and C. W. Slaughter. 1972. Seasonal regime and hydrological significance of stream icings in central Alaska. IAHS **107**: 528–540.

Kane, D. L., K. Yoshikawa, and J. P. McNamara. 2013. Regional groundwater flow in an area mapped as continuous permafrost, NE Alaska (USA). Hydrgeol. J. **21**: 41–52.

Kendrick, M. R., and A. D. Huryn. 2014. The Plecoptera and Trichoptera of the Arctic North Slope of Alaska. West. N. Am. Nat. **74**: 275–285.

Kendrick, M. R., A. E. Hershey, and A. D. Huryn. 2019. Disturbance, nutrients, and antecedent flow conditions affect macroinvertebrate community structure and productivity in an arctic river. Limnol. Oceanogr. **64**: S93–S104.

Kibichii, S., J. R. Baars, and M. Kelley-Quinn. 2009. Optimising sample volume and replicates using the Bou-Rouch method for the rapid assessment of hyporheic fauna. Mar. Freshw. Res. **60**: 83–96.

King, T. V., B. T. Neilson, L. D. Overbeck, and D. L. Kane. 2020. A distributed analysis of lateral inflows in an Alaskan Arctic watershed underlain by continuous permafrost. Hydrol. Process. **34**: 633–648.

Lencioni, V. 2004. Survival strategies of freshwater insects in cold environments. J. Limnol. **63**: 45–55.

Li, S., C. Benson, L. Shapiro, and K. Dean. 1997. Aufeis in the Ivishak River, Alaska, mapped from satellite radar interferometry. Remote Sen. Environ. **60**: 131–139.

Malard, F., D. Ferreira, S. Dolédec, and J. V. Ward. 2003. Influence of groundwater upwelling on the distribution of the hyporheos in a headwater river flood plain. Arch. Hydrobiol. **157**: 89–116.

Manly, B. F. J. 1991. Randomization and Monte Carlo methods in biology. London: Chapman & Hall, London.

Martin, P. D., J. L. Jenkins, F. J. Adams, M. T. Jorgenson, A. C. Matz, D. C. Payer, P. E. Reynolds, A. C. Tidwell, and J. R. Zelenak. 2009. Wildlife response to environmental Arctic change (WildREACH): Predicting future habitats of Arctic Alaska. Fairbanks, AK: U.S. Fish and Wildlife Service.

McNamara, J. P., D. L. Kane, and L. D. Hinzman. 1998. An analysis of streamflow in the Kuparuk River basin, Arctic

Alaska: A nested watershed approach. J. Hydrol. **206**: 39–57.

McNamara, J. P., D. L. Kane, J. E. Hobbie, and G. W. Kling. 2008. Hydrologic and biogeochemical controls on the spatial and temporal patterns of nitrogen and phosphorus in the Kuparuk River, arctic Alaska. Hydrol. Process. **22**: 3294–3309.

Merritt, R., K. Cummins, and M. Berg [eds.]. 2019. An introduction to the aquatic insects of North America, 5th ed. Dubuque, IA: Kendall Hunt.

von Middendorff, A. T. 1867. Reise in den Äussersten Norden und Osten Sibiriens. Band IV. Übersicht der Natur Nord – und Ost – Siberiens. Theil 1. Einleitung, Geographie, Hydrographie, Orographie, Geognosie, Klima und Gewächse. Buchdruckerai der Kaiserlichen Akademie der Wissenshaften, St. Petersburg, Russia.

Nelson, F. E., N. I. Shiklomanov, G. R. Mueller, K. M. Hinkel, D. A. Walker, and J. G. Bockheim. 1997. Estimating active-layer thickness over a large region: Kuparuk River basin, Alaska, USA. Arct. Alp. Res. **29**: 367–378.

Overland, J., J. A. Francis, R. Hall, E. Hanna, S. J. Kim, and T. Vihma. 2015. The melting Arctic and midlatitude weather patterns: Are they connected? J. Climate **28**: 7917–7932.

Parker, S. M., and A. D. Huryn. 2013. Disturbance and productivity as codeterminants of stream food web complexity in the Arctic. Limnol. Oceanogr. **58**: 2158–2170.

Pavelsky, T. M., and J. P. Zarnetske. 2017. Rapid decline in river icings detected in Arctic Alaska: Implications for a changing hydrologic cycle and river ecosystems. Geophys. Res. Lett. **44**: 3228–3235. doi:10.1002/2016GL072397

Poole, G. C., J. A. Stanford, C. A. Frissell, and S. W. Running. 2002. Three-dimensional mapping of geomorphic controls on flood-plain hydrology and connectivity from aerial photos. Geomorphology **48**: 329–347.

Reed, E. B. 1962. Freshwater plankton Crustacea of the Colville River area, northern Alaska. Arctic **15**: 27–50.

Reid, J. W., E. B. Reed, J. V. Ward, N. J. Voelz, and J. A. Stanford. 1991. *Diacyclops languidoides* (Lilljeborg, 1901) s.l. and *Acanthocyclops montana*, new species (Copepoda, Cyclopoida), from groundwater in Montana, USA. Hydrobiologia **218**: 133–149.

Reid, J. W., and D. L. Strayer. 1994. *Diacyclops dimorphus*, a new species of copepod from Florida, with comments on morphology of interstitial cyclopine cyclopods. J. N. Am. Benthol. Soc. **13**: 250–265.

Robertson, A. L., and P. J. Wood. 2010. Ecology of the hyporheic zone: Origins, current knowledge and future directions. Arch. Hydrobiol. **176**: 279–289.

Rothman, K. J. 1990. No adjustments are needed for multiple comparisons. Epidemiology **1**: 43–46.

Sandstrom, S.J. 1995. The effect of overwintering site temperature on energy allocation and life history characteristics of anadromous female Dolly Varden char (*Salvelinus malma*) from northwestern Canada. M.Sc. thesis, Univ. of Manitoba, Winnipeg, Manitoba, Canada.

Savitz, D. A., and A. F. Olshan. 1995. Multiple comparisons and related issues in the interpretation of epidemiologic data. Am. J. Epidemiol. **142**: 904–908.

Schohl, G. A., and R. Ettema. 1990. Two-dimensional spreading and thickening of aufeis. J. Glaciol. **36**: 169–178.

Sokolov, B. L. 1991. Hydrology of rivers of the cryolithic zone in the U.S.S.R.: The present state and prospects for investigations. Nord. Hydrol. **22**: 211–222.

Sokolov, B.L. 1973. Regime of naleds. USSR Academy of Sciences, Earth Sciences Section, Siberian Branch, Second International Conference on Permafrost, Lectures and Reports 5: 68-74. Yakutsk Book Publishing Co., Yakutsk, Russia.

Stanford, J. A., and A. R. Gaufin. 1974. Hyporheic communities of two Montana rivers. Science **185**: 700–702.

Stanford, J. A., J. V. Ward, and B. K. Ellis. 1994. Ecology of the alluvial aquifers of the Flathead River, Montana, p. 367–390. *In* J. Gibert, D. L. Danielopol, and J. A. Stanford [eds.], Groundwater ecology. San Diego, CA: Academic Press.

Stanley, E. H., and A. J. Boulton. 1993. Hydrology and the distribution of hyporheos: Perspectives from a Mesic river and a desert stream. J. N. Am. Benthol. Soc. **12**: 79–83.

Stewart, K. W., and M. W. Oswood. 2006. The stoneflies (Plecoptera) of Alaska and western Canada. Columbus, OH: The Caddis Press.

Strayer, D. L., S. E. May, P. Nielsen, W. Wollheim, and S. Hausam. 1997. Oxygen, organic matter, and sediment granulometry as controls on hyporheic animal communities. Arch. Hydrobiol. **140**: 131–144.

Tash, J. C. 1971. Crustacean zooplankton of the Noatak River area, northern Alaska. Arctic **24**: 108–112.

Terry, N. C., E. Grunewald, M. A. Briggs, M. Gooseff, A. D. Huryn, M. A. Kass, K. Tape, P. Hendrickson, and J. W. Lane Jr. 2019. 2016–2017 geophysical data from the Kuparuk aufeis. North Slope, AK: U.S. Geological Survey data release. doi:https://doi.org/10.5066/F7833R9D

Terry, N. C., E. Grunewald, M. Briggs, M. Gooseff, A. D. Huryn, M. A. Kass, K. Tape, P. Hendrickson, and J. W. Lane Jr. 2020. Seasonal subsurface thaw dynamics of an aufeis feature inferred from geophysical methods. J. Geophys. Res. Earth Surf. **125**. doi:10.1029/2019JF005345

Bureau of Reclamation. 1995. Ground water manual: A guide for the investigation, development, and management of ground-water resources. Washington, DC: Water Resources Technical Publication, U.S. Government Printing Office.

Ward, J. V., and N. J. Voelz. 1990. Gradient analysis of interstitial meiofauna along a longitudinal stream profile. Stygologia **5**: 93–99.

Ward, J. V., and N. J. Voelz. 1994. Groundwater fauna of the South Platte River system, Colorado, p. 391–425. *In* J. Gibert, D. L. Danielopol, and J. A. Stanford [eds.], Groundwater ecology. San Diego, CA: Academic Press.

Williams, D. D. 1993. Changes in freshwater meiofauna communities along the groundwater-hyporheic water ecotone. Trans. Am. Microsc. Soc. **112**: 181–194.

Woessner, W. W. 2017. Hyporheic zones, p. 129–157. *In* F. R. Hauer and G. A. Lamberti [eds.], *Methods in stream ecology, 3rd Edition. Volume 1: Ecosystem structure*. San Diego, CA: Academic Press.

Yoshikawa, K., L. D. Hinzman, and D. L. Kane. 2007. Spring and aufeis (icing) hydrology in Brooks Range, Alaska. J. Geophys. Res. **112**: G04S43. doi:10.1029/2006JG000294

Zhang, T. 2011. Talik, p. 1143–1144. *In* V. P. Singh, P. Singh, and U. K. Haritashya [eds.], The encyclopedia of snow, ice and glaciers. Dordrecht, The Netherlands: Springer.

Zarnetske, J. P., M. N. Gooseff, W. B. Bowden, M. J. Greenwald, T. R. Brosten, J. H. Bradford, and J. P. McNamara. 2008. Influence of morphology and permafrost dynamics on hyporheic exchange in arctic headwater streams under warming climate conditions. Geophys. Res. Lett. **35**: L02501. doi:10.1029/2007GL032049

Acknowledgments

We thank Victoria Rahming, Keeton Molt, Scott McCollum and Emmett Webb (Pollux Aviation) for safe helicopter transportation to the Kuparuk aufeis field. We also thank Carla L. Atkinson, Gina Lupo, Mike Kendrick and Anne Bell (University of Alabama), Frances Ianucci (University of Vermont), and Eric White (U.S. Geological Survey, USGS). Maria H. Huryn provided a translation of von Middendorff (1867). Daniel McEwan (Limnopro Aquatic Science) provided identifications of the microcrustacea and Seth Tyler (University of Maine, Orono) provided identifications of the Turbellaria. Jonathan P. Benstead (University of Alabama), Joshua C. Koch (USGS, Anchorage, Alaska), Ryan A. Sponseller (Umeå University, Umeå, Sweden), and two anonymous reviewers provided helpful criticism of an earlier version of this paper. Funding was provided by the U.S. National Science Foundation (OPP-1503868, OPP-1504453, and DEB-1637459). Any use of trade, firm, or product names is for descriptive purposes only and does not imply endorsement by the U.S. Government.

Conflict of Interest

None declared.

Submitted 06 May 2020
Revised 23 August 2020
Accepted 19 September 2020

Associate editor: Ryan Sponseller